

Analysis of a Phase-Locked Loop to Suppress Interference from a Solar Power Satellite

J.R. Juroshek

F.G. Stewart



U.S. DEPARTMENT OF COMMERCE
Malcolm Baldrige, Secretary

Dale N. Hatfield, Acting Assistant Secretary
for Communications and Information

February 1981



TABLE OF CONTENTS

	Page
LIST OF FIGURES	iv
LIST OF TABLES	v
ABSTRACT	1
1. INTRODUCTION	1
2. PHASE-LOCKED LOOPS	4
3. PERFORMANCE ESTIMATES	7
4. AMPLITUDE VARIATION	16
5. CONCLUSIONS	16
6. ACKNOWLEDGEMENT	17
7. REFERENCES	17

LIST OF FIGURES

		Page
Figure 1.	Block diagram of interference cancellation	3
Figure 2.	Block diagram of phase-locked loops. Synchronous version in 2(b) assumes phase-lock has been achieved	5
Figure 3.	Simulation results for an input phase function of $\phi_i(t) = 2\pi 50t$ and loop gain of $k = 2\pi 10^3$	10
Figure 4.	Simulation results for an input phase function of $\phi_i(t) = \cos 2\pi 20t$ and loop gain of $k = 2\pi 10^3$	11
Figure 5.	Simulation results for an input phase function of $\phi_i(t) = 4\cos 2\pi 5t$ and loop gain of $k = 2\pi 10^3$	12
Figure 6.	Simulation results for an input phase function of $\phi_i(t) = \cos(2\pi 20t) + 2\pi 50t$ and loop gain of $k = 2\pi 10^3$	13
Figure 7.	Simulation results for an input phase function of $\phi_i(t) = \cos 2\pi$ and loop gain of $k = 2\pi 10^4$	14

LIST OF TABLES

		Page
Table 1.	Expected field intensities at the surface of the earth from a single 2.45 GHz SPS	2
Table 2.	Performance equations for an order 2, type 1, phase-locked loop with a loop filter of $H_2(s) = \frac{(s + 1)}{a} / \frac{(s + 1)}{b}$	6
Table 3.	Signal level estimates at the input to a phase-locked loop	7
Table 4.	Summary of phase-locked loop characteristics and simulation parameters	9

ANALYSIS OF A PHASE-LOCKED LOOP TO SUPPRESS
INTERFERENCE FROM A SOLAR POWER SATELLITE

J. R. Juroshek and F. G. Stewart^{*}

Interference to radio receivers, such as those used in radio astronomy, can present problems. Adding conventional filters to a radio astronomy receiver's input generally results in an appreciable increase in noise temperature if the filters have any significant losses or if they are not cryogenically cooled. This report takes a cursory look at the possibility of using signal cancellation techniques as an alternate method for eliminating interference in these cases. The technique is particularly suited to interference from the proposed solar-power satellite which would transmit a coherent, cw, microwave, power signal from a geosynchronous satellite. The analysis concludes that a phase-locked loop and associate AGC circuit could be used to generate a replica of the interfering signal which would then be subtracted from the composite signal. The report also concludes that signal suppression of the order of -30 dB should be possible with current technology.

The report presents a brief analysis of a second-order, type-one, phase-locked loop. Computer simulation of the loop is shown and tracking errors are assessed for various hypothetical SPS phase perturbations. The report concludes that spectral purity of local oscillators and VCO's will be a major factor in determining the amount of signal cancellation possible with such a scheme.

Key words: interference; solar power satellite; phase-locked loops; signal cancellation

1. INTRODUCTION

The feasibility of collecting solar energy in an orbiting geostationary solar power satellite (SPS) and then beaming this energy to earth on a focused microwave beam has received considerable study in recent years. The characteristics of such a system, as currently envisioned, is described in detail in a report by the U.S. Department of Energy (1978). Basically, the satellite would be a 10.4 x 5.2 km array of solar cells that transforms solar energy to direct current (dc) energy. The dc would then be converted to 2.45 GHz microwave energy by an estimated 140,000, 50-kw microwave tubes, and beamed to earth by a 1-km diameter phased array.

Rectification of microwave energy at the earth's surface would be done with a 10 x 13 km antenna that directly converts microwave energy to dc (rectenna). The rectenna is made with panels of 1/2 wave dipoles which are directly connected to rectifiers. It has been estimated that such a system could produce 5 to 10 gigawatts of usable power at the rectenna.

*The authors are with the U.S. Department of Commerce, National Telecommunications and Information Administration, Institute for Telecommunication Sciences, Boulder, Colorado 80303

The electromagnetic compatibility problems associated with the transmission of this amount of microwave energy are considerable. As shown in Table 1, microwave power densities as high as 23 mw/cm^2 can be expected within the boundaries of the $10 \times 13 \text{ km}$ rectenna site. The fields, however, rapidly decrease as one moves away from the rectenna. The fields in Table 1 are for a single SPS satellite, even though current projections are for multiple satellites with a significant overlap of sidelobe radiation patterns. It has been estimated that, with multiple satellites, microwave fields as high as 10^{-4} mw/cm^2 can be expected at average locations in the contiguous United States that are significantly (a few hundred km) removed from an SPS rectenna.

Table 1. Expected power densities and field intensities at the surface of the earth from a single 2.45 GHz SPS.

Center of Rectenna	23 mw/cm^2	294 v/m
Edge of Rectenna (5 km from center)	1.0	61.4
Exclusion Fence (5.7 km from center)	0.1	19.4
First Side Lobe (9.0 km from center)	0.08	17.3
Second Side Lobe (13.0 km from center)	0.03	10.6
Third Side Lobe (17.0 km from center)	0.01	6.1
50 km from Center	.001	1.9
200 km from Center	.0002	.87
400 km from Center	.00005	.43
First Grating Lobe 450 km from Center	.01	6.1

The potential interference problems between SPS and other electronic systems are currently being studied by the U.S. Department of Commerce, NTIA. In addition to identifying these problems, the study is also investigating potential mitigation techniques such as the one described in this report.

Most of the mitigation techniques for SPS are conventional such as increasing the shielding effectiveness of enclosures or adding rf filters to electronic circuits. However, in some instances, such as in radio astronomy, the addition of a filter at a receiver input is not desirable since the losses within a filter,

even though fractional, can result in a significant increase in effective noise temperature. The filters must be cryogenically cooled in order to reduce circuit noise temperatures. The question of concern here is whether or not signal cancellation techniques can be effectively used to decrease interference. This report will briefly examine one such signal cancellation technique.

The problem of concern here is shown in its simplest form in Figure 1. Basically, we would like to construct a circuit that generates an estimate, i_e , of the received interference i . This estimate can then be subtracted from the composite signal to reduce the magnitude of the interference. Any residual error in the process is $\epsilon = i - i_e$, which determines the effectiveness of the technique.

The SPS interfering signal is an ideal candidate for signal cancellation techniques. It is basically a coherent cw signal with modulation components of only a few tens of hertz due to phase and amplitude perturbations acquired in the propagation medium. With interference power densities of 10^{-4} to 10^{-6} mw/cm^2 , the SPS signal is significantly stronger than thermal noise or cosmic noise in comparable bandwidths. In the case of radio astronomy, the interference is also many orders of magnitude greater than the signal, which is typically of the order of -306 dB ($\text{w/m}^2 \cdot \text{Hz}$) (CCIR Report 224-4, 1978).

Obviously a number of estimation techniques exist. The purpose of this paper is not to provide an optimum technique, but only to examine the potential of one specific circuit, a phase-locked loop. The following discussion will present a brief tutorial of phase-locked loop in order to provide estimates of the amount of signal cancellation possible with such a technique.

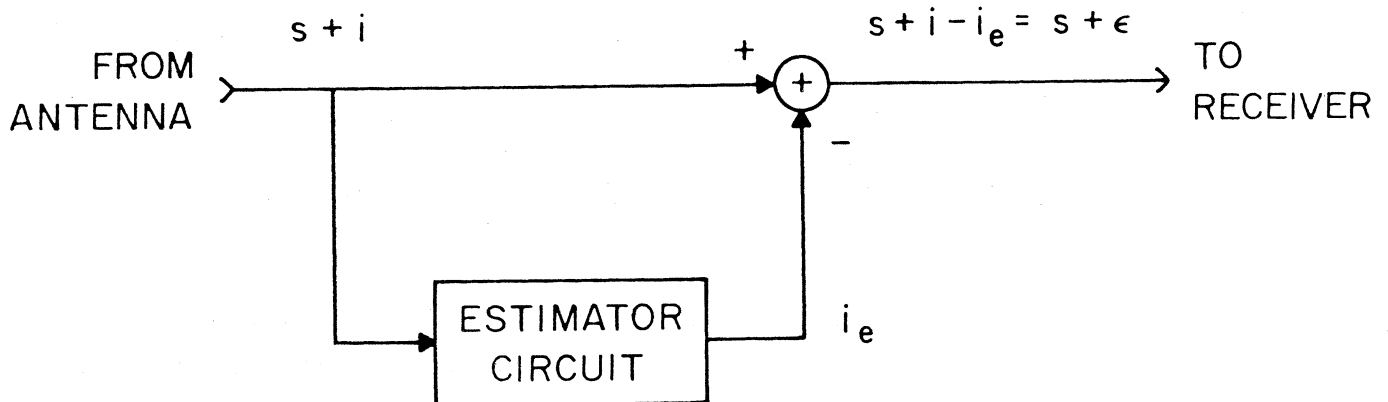


Figure 1. Block diagram of interference cancellation

2. PHASE-LOCKED LOOPS

Phase-locked loops have been used for a number of years to separate phase coherent signals from noise or other types of noncoherent signals. A prime example is in the field of communications where phase-locked loops are used to detect suppressed carriers that are often 30 dB or more weaker than the modulation components. Phase-locked loops can also be used as narrowband tracking filters providing bandwidths of only a few hertz (Moschytz, 1965). The following material will discuss some of the basic principles involved in phase locked loops, and provide estimates of the phase tracking accuracy available from such loops.

The theory of phase locked loops is treated in a number of text books (Blanchard, 1976; Klapper and Frankle, 1972). The basic loop as shown in Figure 2(a) consists of a phase detector, a loop filter and amplifier, and voltage controlled oscillator (VCO). The phase detector is assumed to be an ideal multiplier detector that produces an output proportional to the difference in phase of the input signals or $\sin [\phi_i(t) - \phi_r(t)]$ where $\phi_i(t)$ and $\phi_r(t)$ are defined in the figure. All double frequency terms at $2\omega_i$ are assumed to be effectively eliminated by filtering within the phase detector.

The Laplace transform of the loop filter is defined as $K_2 H_2(s)$ where K_2 is a gain constant and $H_2(s)$ is the normalized filter transfer function. The voltage controlled oscillator, whose instantaneous frequency is varied with the applied signal, is defined by

$$e_r(t) = -\frac{2}{A} \sin \left[\omega_i t + K_2 \int_0^t e_c(\tau) d\tau \right],$$

where $e_c(t)$ is the input control voltage. Frequency deviation is determined by the VCO sensitivity constant K_3 with units of radians per volt-second.

Although there are many choices for a loop filter, this report will be primarily concerned with a filter of the form

$$H_2(s) = \frac{\left(\frac{s}{a} + 1\right)}{\left(\frac{s}{b} + 1\right)}$$

which is classified in the literature as a filter of order 2 and type 1. This form of filter function was chosen since it is relatively simple and demonstrates major principles, but yet retains some of the design flexibility of the more complex loop filters. One of the major advantages of this type of loop is that the hold-in range and loop bandwidth can be designed independently. A disadvantage is that this loop has a greater tendency to become unstable with the addition of parasitic elements.

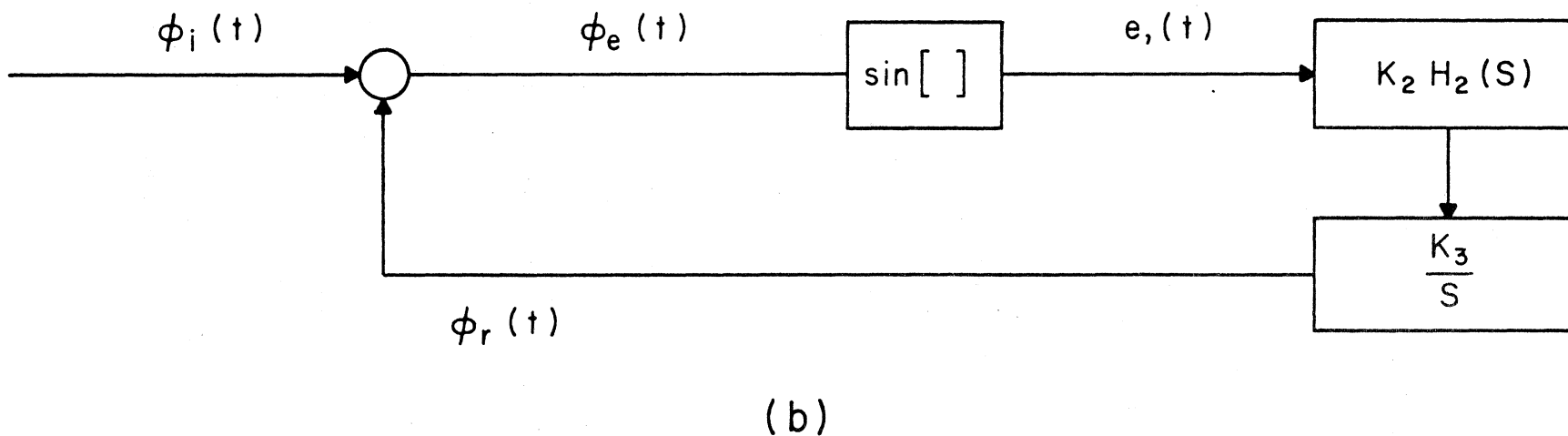
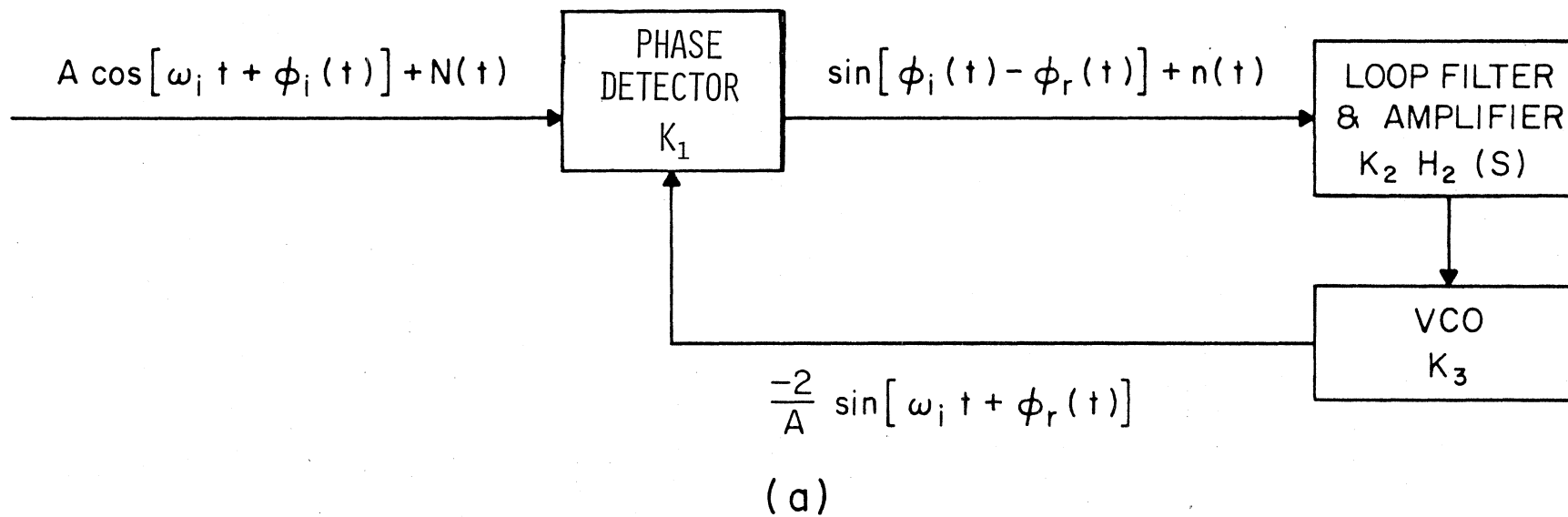


Figure 2. Block diagram of phase-locked loops. Synchronous version in 2(b) assumes phase-lock has been achieved

The major equations describing the performance of the loop are given in Table 2. Of particular interest here is the equation for the tracking error $\phi_e(t) = \phi_i(t) - \phi_r(t)$ when the input is perturbed by a unit step in frequency

Table 2. Performance equations for an order 2, type 1, phase-locked loop with a loop filter of $H_2(s) = (\frac{s}{a} + 1) / (\frac{s}{b} + 1)$

Loop Gain	$K = K_1 K_2$ rad/volt-sec
Loop Natural Frequency	$\omega_n = (Kb)^{1/2}$ rad/sec
Damping Factor	$\zeta = \frac{1}{2} \left(\frac{b}{K}\right)^{1/2} + \frac{(Kb)^{1/2}}{2a}$
Pull in Range	$\Delta\omega_i < 2 \left[Kb \left(1 + \frac{1}{2} \frac{K}{a}\right) \right]^{1/2}$ rad/sec
Hold in Range	$\Delta\omega_i \leq KH_2(0)$ rad/sec
Pull in Time	$\tau = a(\Delta\omega_i / Kb)^2$ sec
Loop Noise Bandwidth	$B_n = \frac{Kb \left(\frac{Kb}{a} + a\right)}{4a \left(\frac{Kb}{a} + b\right)}$ rad/sec
Tracking Error for Unit Step in Input Frequency $\phi_i(t) = (\Delta\omega_i t + \phi_{i0}) u(t)$	$\lim_{t \rightarrow \infty} \phi_e(t) = \frac{\Delta\omega_i}{K}$

of

$$\phi_i(t) = (\Delta\omega_i t + \phi_{i0}) u(t).$$

The unit step function $u(t)$ is defined by

$$u(t) = \begin{cases} 1 & t \geq 0 \\ 0 & t < 0 \end{cases}.$$

As can be seen, the error in the limit approaches

$$\lim_{t \rightarrow \infty} \phi_e(t) = \frac{\Delta\omega_i}{K}.$$

Note that the limiting error can be made arbitrarily small by increasing loop gain K . The implications of this equation will be seen in more detail in the following material.

A second model of a phase locked loop is the synchronous model as shown in Figure 2(b). The major difference in this model is that it is valid only after synchronization has been achieved. Thus the input to the model is the input phase perturbations $\phi_i(t)$. Also note that the VCO is specified by an ideal integrator of K_3/s .

3. PERFORMANCE ESTIMATES

The performance of a cancellation scheme is dependent on the phase-tracking accuracy of the phase-locked loop. Tracking accuracy, on the other hand, is determined by various parameters such as loop design, component stability, and circuit noise. The following will show that phase-tracking errors due to circuit noise can be expected to be quite low in relationship to other errors. This is a contrast to the normal situation with phase-locked loops, which often track signals under poor signal-to-noise conditions.

An estimate of the signal-to-noise ratio that can be expected in the phase-locked loop bandwidth is shown in Table 3. This estimate assumes a typical SPS signal level at the aperture of the victim antenna of 10^{-6} or 10^{-4} mw/cm^2 . Also assumed is that the victim antenna presents an aperture to the SPS signal of $\lambda^2/4\pi$ where λ is the SPS wavelength of 12.2 cm. These assumptions mean that the effective aperture of the victim antenna to the interfering SPS signal is at least equivalent to an isotropic radiator. One can conclude from this exercise that the thermal noise at the input to the loop is not likely to be the major source of phase-tracking error. Tracking error is more likely to be determined by VCO instabilities and other loop design considerations.

Table 3. Signal level estimates at the input to a phase-locked loop

SPS interfering signal level	10^{-6} mw/cm^2	10^{-4} mw/cm^2
Victim antenna aperture	11.8 cm^2	11.8 cm^2
SPS signal level at antenna terminals	-79 dBw	-59 dBw
Effective system noise temperature referenced to antenna terminals	100°K	100°K
Noise power density, KT	-208 dBw/Hz	-208 dBw/Hz
Signal-to-noise power density at input to loop	129 dB/Hz	149 dB/Hz
Loop equivalent noise bandwidth, Bn	1×10^3 Hz	1×10^3 Hz
Signal-to-noise ratio in loop equivalent bandwidth	99 dB	119 dB

In order to demonstrate the effects of loop design on tracking error, a computer program was constructed that simulated the synchronous loop model shown in Figure 2(b). A special computer simulation language was used that computes the dc transient, and ac response of electrical circuits (Becker, 1974). This type of simulation language provides a convenient method for obtaining the response of circuits under ideal,

controllable conditions. Inputs to the program can be in the form of circuit components or Laplace transfer functions such as described in Figure 2.

The simulation was carried out for five hypothetical examples in order to demonstrate the principles involved. The constants for the loop filter $H_2(S)$ were chosen as

$$a = 2\pi 50 \text{ radians}$$

and

$$b = 2\pi 25 \text{ radians.}$$

Loop gain K was set at either $2\pi \times 10^3$ or $2\pi \times 10^4$ radians/volt-sec in order to demonstrate the effects of increases in this parameter. These constants were selected on the basis that they provide a loop with the reasonable characteristics for tracking an SPS signal. The constants have not been optimized in any manner.

The frequency perturbations due to phase delay and Doppler shifts that are imposed on an SPS signal by the troposphere and ionosphere are generally expected to be of the order of 50 Hz or less. These perturbations are the result of satellite motion as well as perturbations in the propagation path due to the ionosphere and troposphere. It is possible for greater frequency perturbations to occur in certain scenarios. For example, a reflection from an aircraft moving 268 m/sec (600 mi/hr) would generate a 2.2 kHz maximum Doppler shift at 2.45 GHz. However, such extremes are not likely in practice because the geometry of the situation is likely to produce Doppler shift much less than the maximum. This report will assume maximum frequency perturbations of the order of 50 Hz. During the computer simulations, input phase perturbations $\phi_i(t)$ were arbitrarily selected as

$$(a) \quad \phi_i(t) = 2\pi 50t \quad \text{rad,}$$

$$(b) \quad \phi_i(t) = \cos 2\pi 20t \quad \text{rad,}$$

$$(c) \quad \phi_i(t) = 4\cos 2\pi 5t \quad \text{rad,}$$

$$(d) \quad \phi_i(t) = \cos(2\pi 20t) + 2\pi 50t \quad \text{rad.}$$

The frequency perturbation produced by each of these functions is $\Delta\omega_i = \frac{d\phi_i(t)}{dt}$ or

$$(a) \quad \Delta\omega_i = 2\pi 50 \text{ rad/sec,}$$

$$(b) \quad \Delta\omega_i = -2\pi 20 \sin 2\pi 20t \text{ rad/sec,}$$

$$(c) \quad \Delta\omega_i = -2\pi 20 \sin 2\pi 5t \text{ rad/sec,}$$

$$(d) \quad \Delta\omega_i = -2\pi 20 \sin(2\pi 20t) + 2\pi 50 \text{ rad/sec.}$$

Thus, the phase function specified in (a) corresponds to a constant 50 Hz shift in the SPS signal. Functions (b) and (c), on the other hand, produce a signal with a cosine frequency modulation and peak frequency deviation of ± 20 Hz. The difference between (b) and (c) is the frequency deviation rate. In (b), the frequency deviation takes place at a 20 Hz, while (c) has a 5 Hz rate. Finally, the function in (d) combines a cosine frequency modulation with a fixed 50 Hz offset.

A summary of the loop characteristics that can be expected for these design conditions is given in Table 4. Each of these examples was simulated to further demonstrate the principles involved. Simulation results are shown in Figures 3 through 7. Note that the simulation tracking errors generally agree with the predicted errors shown in the last line of Table 4. Figure 3 shows that a constant frequency offset produces a constant phase-tracking error. Figures 4 and 5, on the other hand, show that frequency modulation of the input signal produces a corresponding oscillation in the phase error.

Table 4. Summary of phase-locked loop characteristics and simulation parameters

$\phi_i(t)$, rad	$2\pi 50t$	$\cos(2\pi 20t)$	$4\cos(2\pi 5t)$	$\cos(2\pi 20t)+2\pi 50t$	$\cos(2\pi 20t)$
a	$2\pi 50$	$2\pi 50$	$2\pi 50$	$2\pi 50$	$2\pi 50$
b	$2\pi 25$	$2\pi 25$	$2\pi 25$	$2\pi 25$	$2\pi 25$
K	$2\pi 10^3$	$2\pi 10^3$	$2\pi 10^3$	$2\pi 10^3$	$2\pi 10^4$
ω_n $\frac{\text{rad}}{\text{sec}}$	$2\pi 158$	$2\pi 158$	$2\pi 158$	$2\pi 158$	$2\pi 500$
ξ	1.6	1.6	1.6	1.6	5.0
PULL IN RANGE, rad/sec	$2\pi 10^3$	$2\pi 10^3$	$2\pi 10^3$	$2\pi 10^3$	$2\pi 10^4$
HOLD IN RANGE, rad/sec	$2\pi 10^3$	$2\pi 10^3$	$2\pi 10^3$	$2\pi 10^3$	$2\pi 10^4$
B_n , rad/sec	$2\pi 125$	$2\pi 125$	$2\pi 125$	$2\pi 125$	$2\pi 1250$
$\lim_{t \rightarrow \infty} e(t)$, rad	0.05	0.02	0.02	0.07	0.002

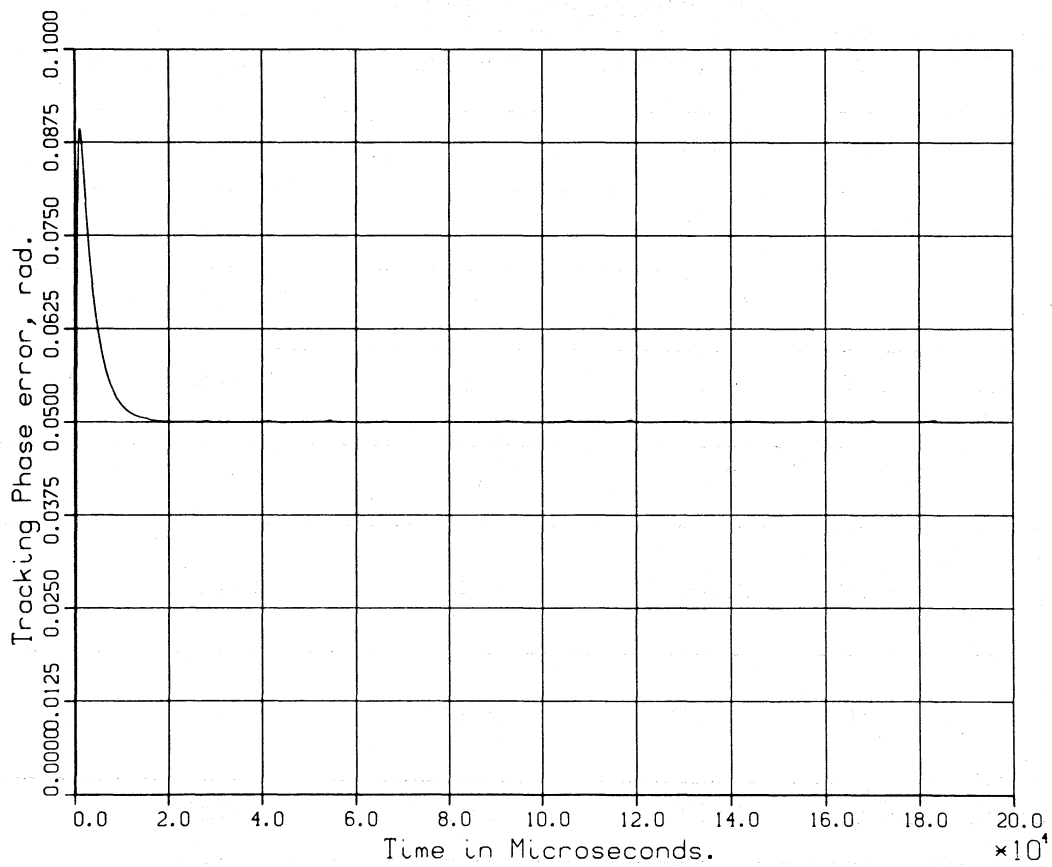
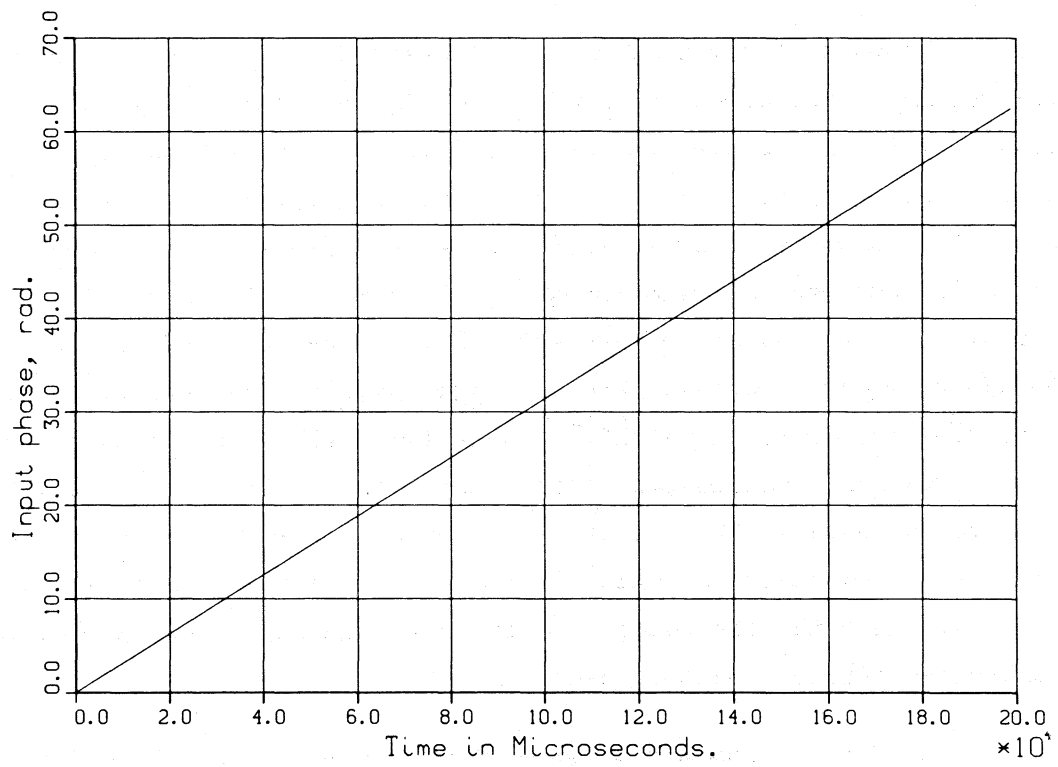


Figure 3. Simulation results for an input phase function of $\phi_i(t) = 2\pi 50t$ and loop gain of $k = 2\pi 10^3$

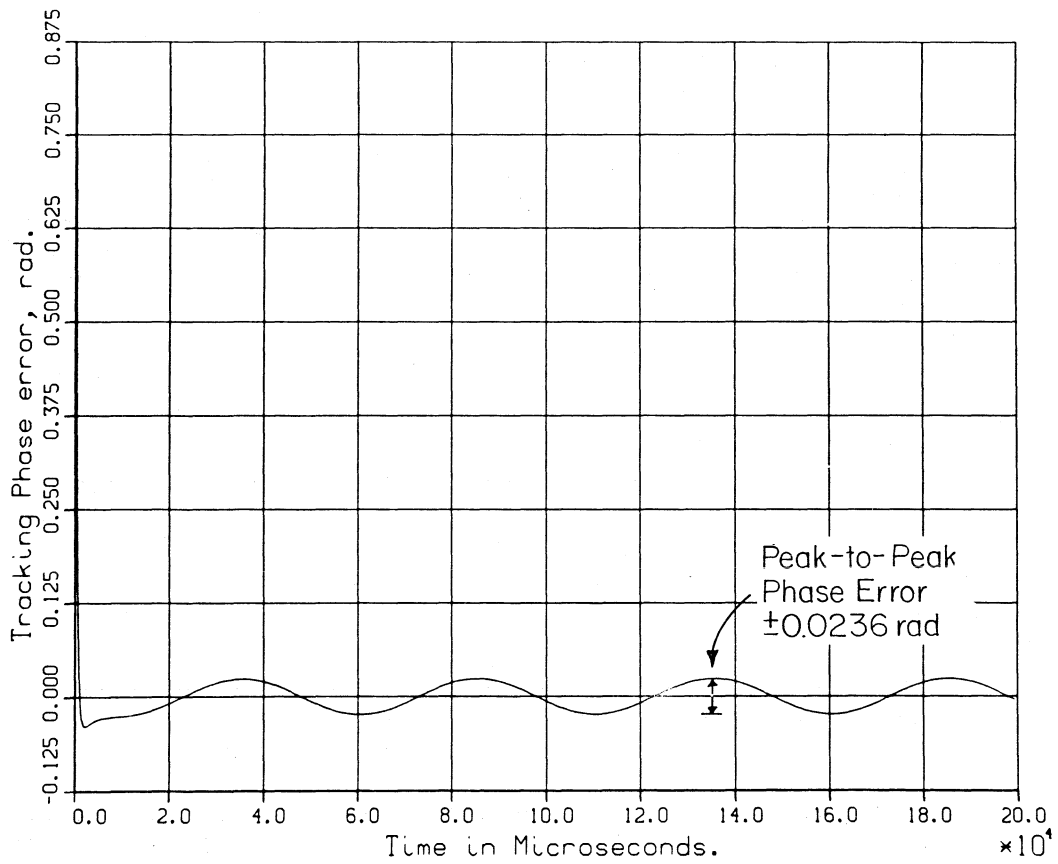
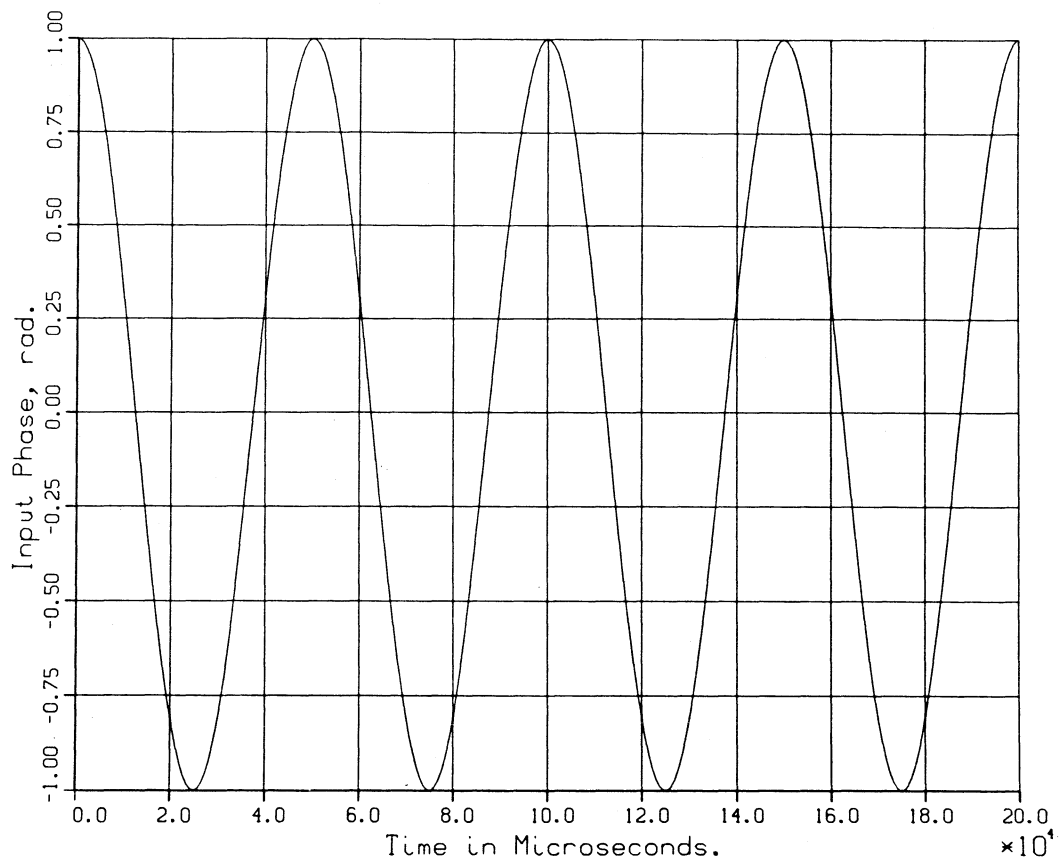


Figure 4. Simulation results for an input phase function of $\phi_i(t) = \cos 2\pi 20t$ and loop gain of $k = 2\pi 10^3$

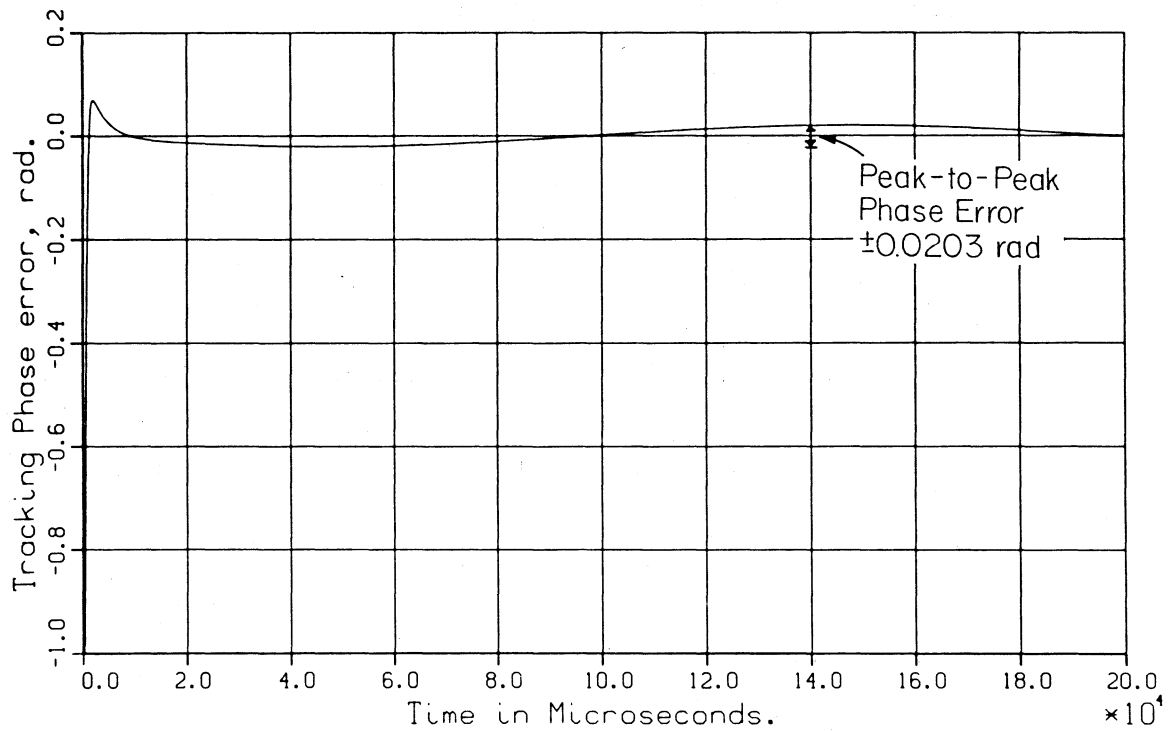
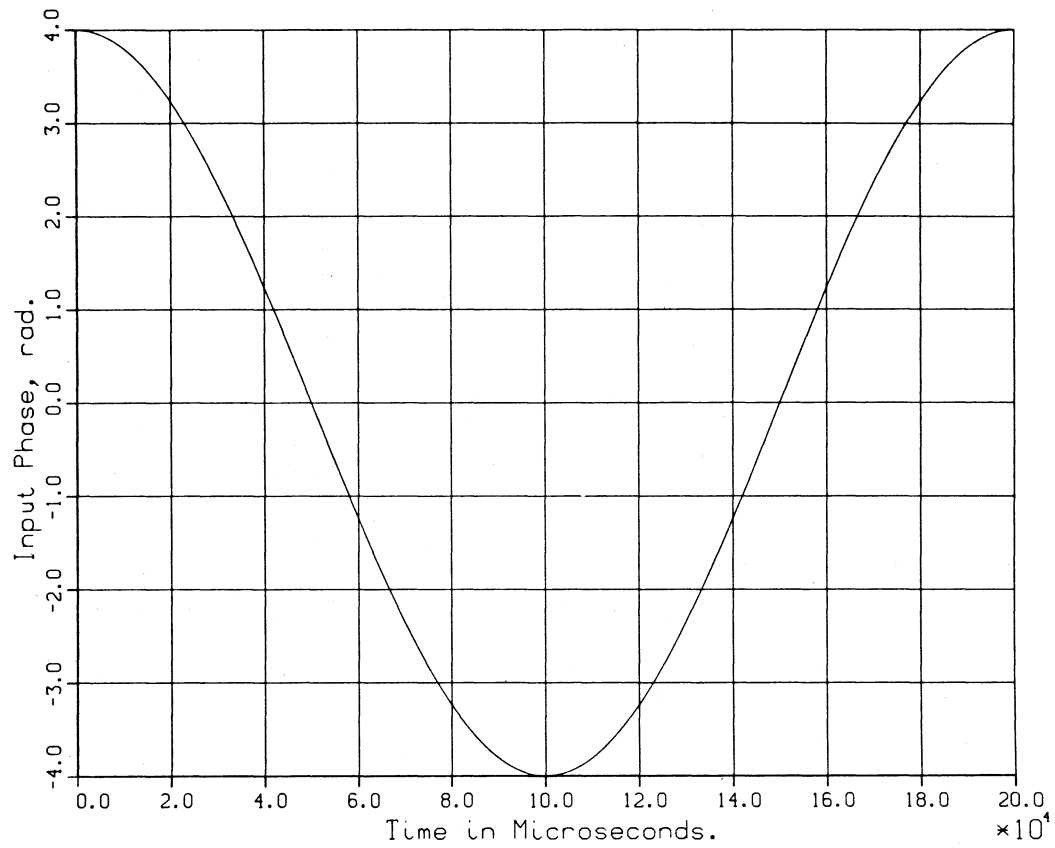


Figure 5. Simulation results for an input phase function of $\phi_i(t) = 4\cos 2\pi 5t$ and loop gain of $k = 2\pi 10^3$

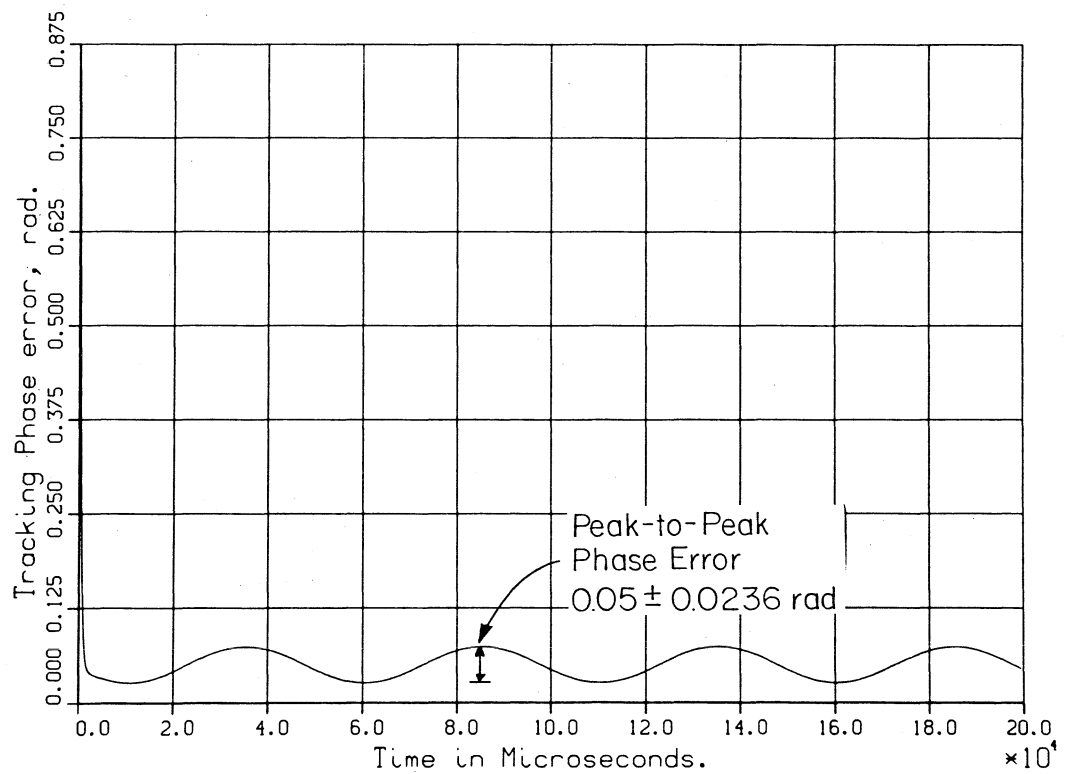
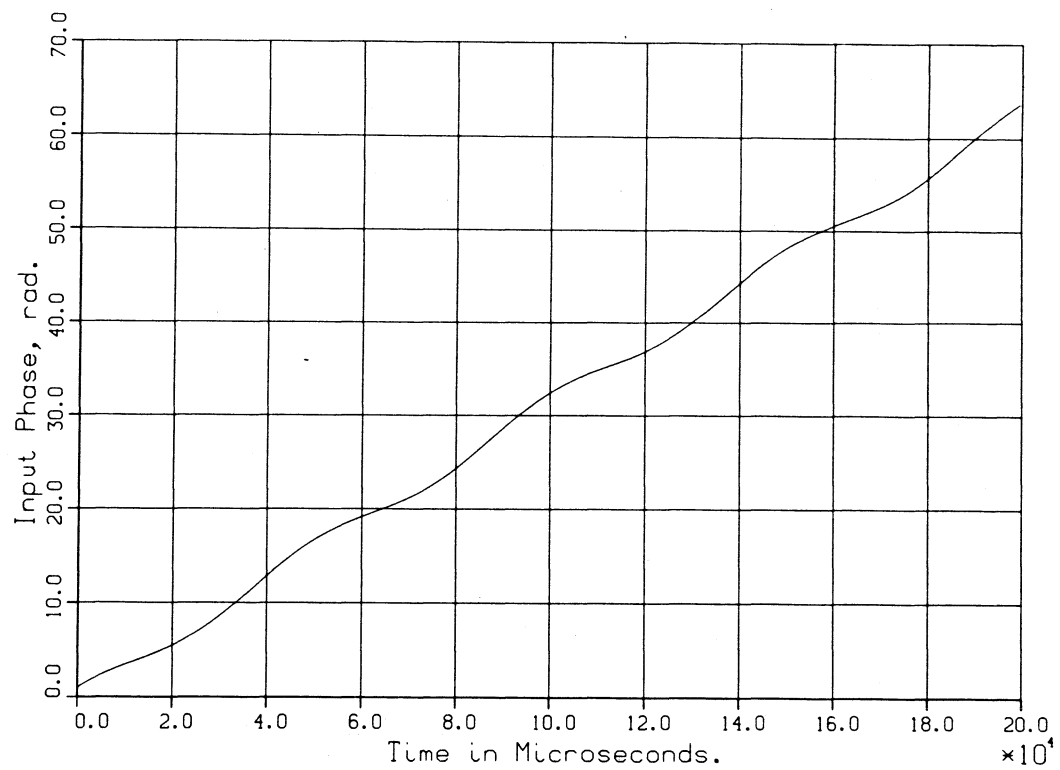


Figure 6. Simulation results for an input phase function of $\phi_i(t) = \cos(2\pi 20t) + 2\pi 50t$ and loop gain of $k = \frac{1}{2}\pi 10^3$

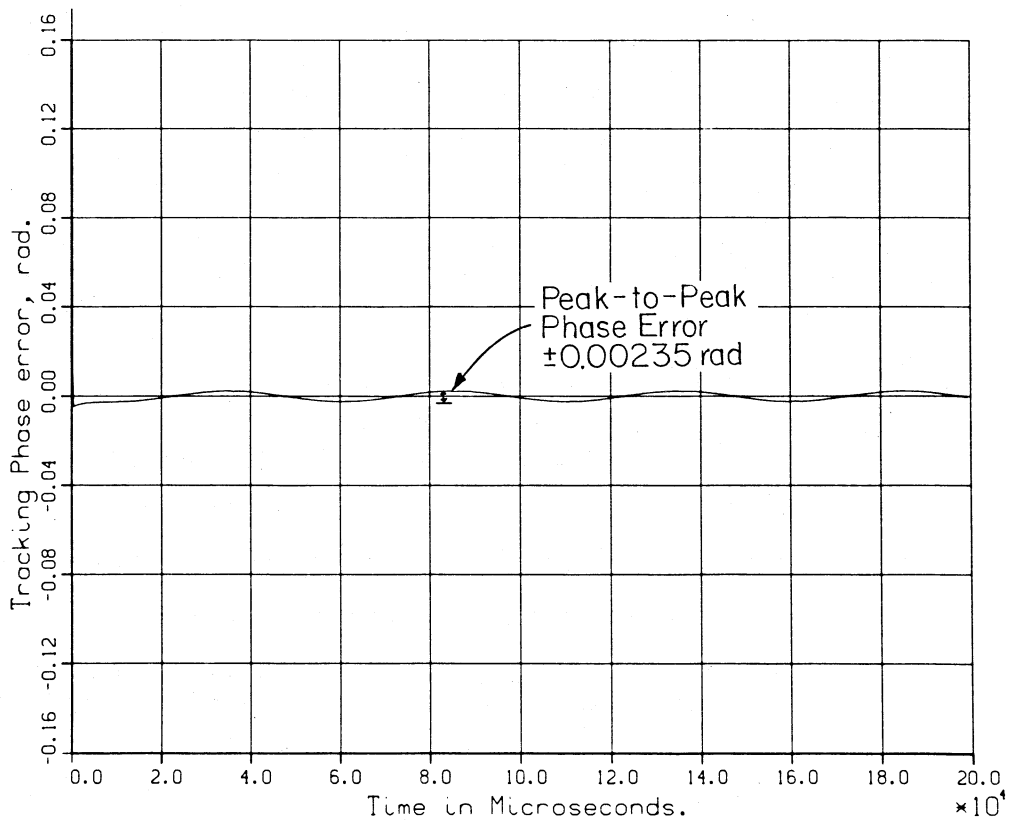
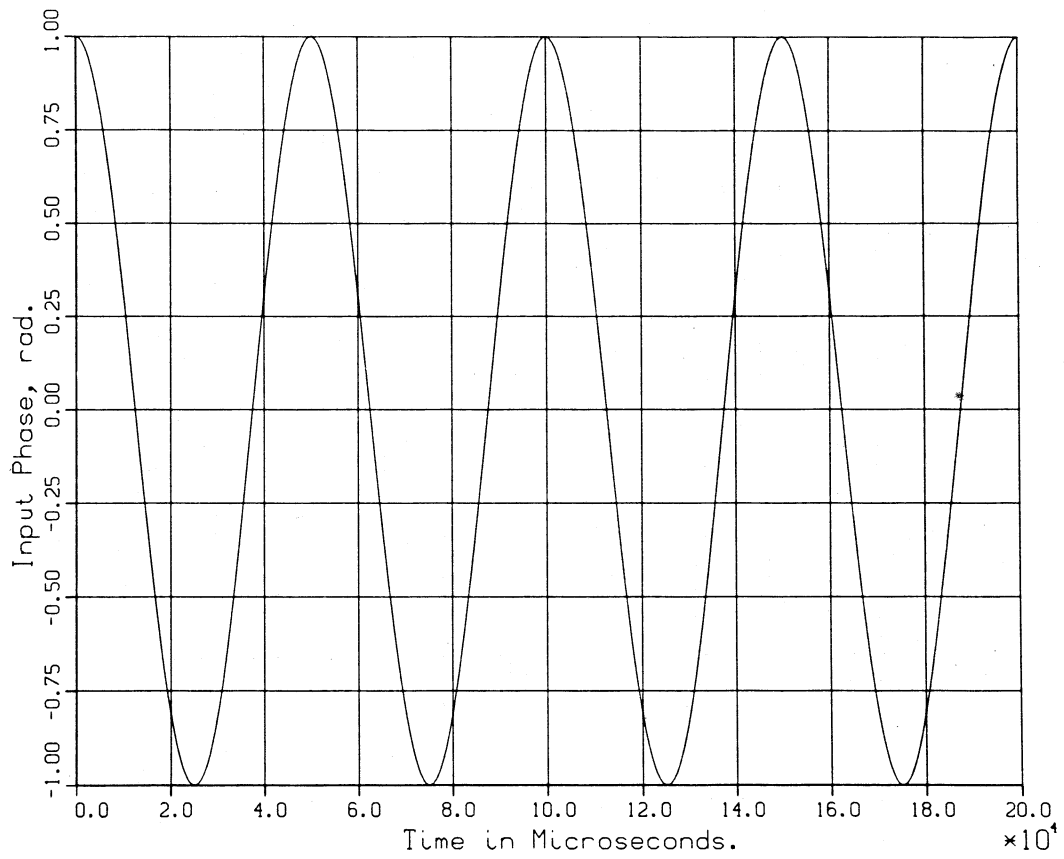


Figure 7. Simulation results for an input phase function of $\phi_i(t) = \cos 2\pi t$ and loop gain of $k = 2\pi 10^4$

The magnitude of the phase-tracking error in each of these cases generally agrees with the predictions in Table 4. In Figure 3, the simulation results correspond exactly with the predicted value. The predicted phase error in Table 4 was approximately ± 0.02 radians, while the simulation results in Figure 4 showed ± 0.0236 radians. The reason for this discrepancy is that the predictions are for a unit step in frequency while the simulation was for a sinusoidal frequency modulation of the input signal. Modulation rate and function are important since they affect the loops tracking ability. This is demonstrated in Figure 5 where the input frequency to the loop is modulated ± 20 Hz, but at a 5 Hz rate as opposed to the 20 Hz rate used in Figure 4. Note that the peak error decreases from ± 0.0236 radians to ± 0.0203 radians. Figure 6 shows that a sum of the preceding events produces an error function that is the sum of individual errors. The last example in Figure 7 shows that the tracking error can be reduced by increasing the loop gain. The error decreased from ± 0.0236 radians, as shown in Figure 4, to ± 0.00236 radians with an increase in K from $2\pi 10^3$ to $2\pi 10^4$.

So far the discussion has not considered any tracking errors induced by VCO instabilities. Consider for the moment a VCO with a frequency stability of 1 part in 10^7 . If the VCO had a operating frequency of 2.45 GHz, the frequency instabilities would amount to 245 Hz. Clearly, a VCO of this caliber would not be able to track SPS frequency changes of the order of a few Hertz. Tracking a frequency change of 1 Hz at 2.45 GHz would require an accuracy of 4 parts in 10^{10} . Although this degree of accuracy is not available in VCO's, it is available in high quality frequency sources. This is fortunate since it allows the possibility of coherently mixing the SPS signal using a high stability local oscillator to a lower frequency where phase synchronization can be achieved with the lower stability VCO's.

The phase noise associated with current high quality, gigahertz frequency synthesizers is fairly high. For example, the ratio of power in the phase noise component relative to the signal is typically of the order of -30 to -40 dB. Phase noise here is measured in a bandwidth of 1 to 100 Hz adjacent to the carrier. Phase noise of this magnitude corresponds to phase perturbations of the order of .03 to .01 radians. With phase noise of this magnitude, the phase noise associated with such oscillators would be a significant factor in determining tracking errors.

The loops described in this section have not been optimized in terms of achieving a minimum noise bandwidth. A damping factor of $\xi = 1$ is generally desirable in order to achieve a minimum noise bandwidth. Although the value of $K = 2\pi 10^3$ provides a ξ of 1.6, the final loop design could probably be improved with proper optimization of parameters.

4. AMPLITUDE VARIATION

So far the discussion has avoided any discussion of amplitude variations in the SPS signal. Amplitude variations can be caused by various factors such as rain storms that cross the path or reflections from aircraft that suddenly enter the path. Amplitude variations can also be caused by the interaction of two adjacent SPS signals. Currently it is not known if adjacent SPS satellites would be phase locked together. If they were, amplitude variations would still exist because of the motion of the satellites in their respective orbits. If they were not phase locked, each signal would act independently, which further complicates the signal cancellation circuitry, particularly in those geographical areas where the signals are approximately equal in amplitude. Amplitude tracking of the signal is also necessary so that the cancellation signal can be inserted at the proper amplitude as well as to maintain a constant signal level at the input to the phase-locked loop. A phase-locked loop generally requires that the input signal levels remain constant. Although the magnitude of expected signal variations at typical locations is not known, it is reasonable to expect that it will be greater than 10 dB.

Amplitude variations in a phase-lock loop are tracked and compensated for with conventional AGC (automatic gain control) circuits. A circuit of this type would keep the signal levels at the input to the phase-locked loop constant as well as supply the amplitude estimate for the signal cancellation. While the design of such a circuit is beyond the scope of this limited report, one can observe that AGC amplifiers are, to a large degree, linear devices and hence the signal-to-noise ratio at the output of the device is approximately equal to that at the input. As shown previously, the signal-to-noise ratio at the input can be expected to be as high as 99 dB in an SPS field of 10^{-6} mw/cm². Errors due to AGC circuitry are thus not expected to be a dominate factor.

5. CONCLUSIONS

This preliminary assessment shows that a phase locked loop and associated AGC circuit can be used to suppress interference from a solar power satellite. The devices would provide an amplitude and phase estimate of the interfering signal which could then be used to cancel the interfering signal. The merit of signal cancellation techniques is that it provides a method of reducing interference without resorting to normal filtering techniques. This can be valuable to services such as radio astronomy which can suffer serious losses in sensitivity due to filter losses if these devices are inserted into their receiver input circuits.

The study described in this report is only intended as a cursory look at the problem. Many design details and tradeoffs are required before a working model could be produced. It would also be necessary to compare this technique with other technologies such as cryogenically cooled filters in order to evaluate the advantages and tradeoffs. Further studies should also be prepared to define circuits in greater detail so that more precise performance estimates can be obtained.

The current level of analysis showed that phase-tracking errors of the order of 0.03 radians can be expected. This corresponded to a phase noise of approximately -30 dB relative to the signal. With this level of error, the signal cancellation technique would be only partially effective in that interference components -30 dB from the original signal would still exist. However, even 30 dB of suppression can be useful in some instances, particularly if it prevents overloading or damage to parametric amplifiers or cryogenically cooled FET amplifiers.

The maximum amount of signal suppression available with signal cancellation techniques is not currently known. The costs or advances in technology that would be necessary to improve this figure beyond the estimated 30 dB are also not known. A major factor in improving the signal suppression is obtaining spectrally pure local oscillators and VCO's. In the current design, the spectral purity of the oscillators was believed to be the major obstacle.

Additional information is also needed on the signal parameters in which the circuits can be expected to operate. The amount of frequency shift that can be expected and the amount of amplitude perturbations that can be expected need to be better quantified.

6. ACKNOWLEDGEMENT

The authors wish to acknowledge the support for this investigation provided by the U.S. Department of Energy under the direction of F. A. Koomanoff, Chief, Environmental and Resource Assessment Programs, Solar Technology, Washington, D.C., Contract No. DE-A101-80ER10160.

7. REFERENCES

- Becker, David (1974), Extended sceptre, Vol. I, Report AFWL-TR-73-75, GTE Sylvania, Inc., Needham Heights, MA, (available through U.S. Dept. of Commerce, NTIA, AD/A-009 594), December.
- Blanchard, Alain (1976), Phase-locked loops, applications to coherent receiver design, (John Wiley and Sons, New York).

CCIR Report 224-4 (1978), Characteristics of the radio astronomy service, and interference protection criteria, International Telecommunication Union, XIVth Plenary Assembly, Vol. II, pp. 387-400.

Klapper, Jacob, and John T. Frankle (1972), Phase-locked and frequency-feedback systems, (Academic Press, New York).

Moschytz, G. S. (1965), Miniaturized RC filters using phase-locked loop, BSTJ, May, pp. 823-870.

U.S. Department of Energy (1978), Satellite power system concept development and evaluation program, reference report DOE/ER-0023, Washington, D.C., October.

BIBLIOGRAPHIC DATA SHEET

1. PUBLICATION NO. NTIA Report 81-63		2. Gov't Accession No.	3. Recipient's Accession No.
4. TITLE AND SUBTITLE Analysis of a Phase-Locked Loop to Suppress Interference from a Solar Power Satellite		5. Publication Date February 1981	
		6. Performing Organization Code	
7. AUTHOR(S) J. R. Juroshek and F. G. Stewart		9. Project/Task/Work Unit No.	
8. PERFORMING ORGANIZATION NAME AND ADDRESS National Telecommunications & Information Administration Institute for Telecommunication Sciences 325 Broadway Boulder, CO 80303		10. Contract/Grant No.	
		12. Type of Report and Period Covered	
11. Sponsoring Organization Name and Address U.S. Department of Energy Washington, D.C. 20545		13.	
		14. SUPPLEMENTARY NOTES	
15. ABSTRACT (A 200-word or less factual summary of most significant information. If document includes a significant bibliography or literature survey, mention it here.) Interference to radio receivers, such as those used in radio astronomy, can present problems. Adding conventional filters to a radio astronomy receiver's input generally results in an appreciable increase in noise temperature if the filters have any significant losses or if they are not cryogenically cooled. This report takes a cursory look at the possibility of using signal cancellation techniques as an alternate method for eliminating interference in these cases. The technique is particularly suited to interference from the proposed solar-power satellite which would transmit a coherent, cw, microwave, power signal from a geosynchronous satellite. The analysis concludes that a phase-locked loop and associate AGC circuit could be used to generate a replica of the interfering (Continued next page)			
16. Key Words (Alphabetical order, separated by semicolons) Key words: interference; solar power satellite; phase-locked loops; signal cancellation			
17. AVAILABILITY STATEMENT <input checked="" type="checkbox"/> UNLIMITED <input type="checkbox"/> FOR OFFICIAL DISTRIBUTION		18. Security Class. (This report) UNCLASSIFIED	20. Number of pages 18
		19. Security Class. (This page) UNCLASSIFIED	21. Price:

15. ABSTRACT (Cont.)

signal which would then be subtracted from the composite signal. The report also concludes that signal suppression of the order of -30 dB should be possible with current technology.

The report presents a brief analysis of a second-order, type-one, phase-locked loop. Computer simulation of the loop is shown and tracking errors are assessed for various hypothetical SPS phase perturbations. The report concludes that spectral purity of local oscillators and VCO's will be a major factor in determining the amount of signal cancellation possible with such a scheme.